Hideyuki Tanaka,[1] *Ph.D.; Pete E. Lestrel,*[2] *Ph.D.; Teruo Uetake,*[3] *Ph.D.; Susumu Kato,*[4] *Ph.D.; and Fumio Ohtsuki,*[5] *Ph.D.*

Sex Differences in Proximal Humeral Outline Shape: Elliptical Fourier Functions

REFERENCE: Tanaka H, Lestrel PE, Uetake T, Kato S, Ohtsuki F. Sex differences in proximal humeral outline shape: elliptical Fourier functions. J Forensic Sci 2000;45(2):292–302.

ABSTRACT: A method is presented for the numerical analysis of sex differences in size and shape of the proximal humeral outlines using elliptical Fourier functions (EFFs). A skeletal sample consisting of right and left humeri pairs of 69 individuals, 36 males and 33 females, was used. The proximal superior view in the plane of the proximo-distal axis of each humerus was photographed and then 54 boundary points were located on the two-dimensional outline tracings. These points were digitized and used to compute EFFs with 27 harmonics. From the EFFs, a set of expected points on the proximal humeral outline was generated using the centroid as an origin. Superimposition of the male and female outlines on this centroid provided a detailed picture of the relative sex differences in size and shape with respect to that center.

The bounded area of the proximal humeral outline showed statistically significant sex differences. Additionally, statistical results of the amplitudes derived from the "area-standardized" EFFs and visual assessments of the mean outline plots indicated significant sex differences in shape of the proximal humeral outlines. Focusing on localized regional differences, the greater tubercle was located more postero-medially and the lesser tubercle was located more anteriorly in the males compared to the females. Sex determinations from the proximal humeri were also examined with discriminant functions based on the amplitudes, which represent shape characteristics of the outline, and the bounded area. Using a cross-validation method, predictions of the percentages of cases correctly classified with the discriminant functions were ranged from 92.8% to 95.7% for the right and left humeral data. These results suggest that differences in size and shape of the proximal humeral outlines may be better predictors of sex when compared with conventional measurements of the humerus.

KEYWORDS: forensic science, human morphology, photogrammetry, Japanese, sexual dimorphism, discriminant function analysis

Many parts of the human skeleton show remarkable sexual dimorphism. Sex differences in the skeletal morphology have been studied by many investigators focusing on the assessment of sex in unidentified skeletal remains. In many cases, particularly those involving an intact cranium and pelvis, qualitative morphological observations may be sufficient for accurate sex identification (1). Recently, multivariate statistical techniques such as discriminant function analysis have been widely used for sex determinations. Although with a somewhat lower accuracy, sex has been quantitatively determined with discriminant functions based on diverse skeletal regions. These included the calcaneus and talus (2); pelvis (3,4); tibia (5,6); radius and ulna (1); and femur (7,8). The measurements employed in the above discriminant function studies were based on the conventional metrical approach (CMA) consisting of distances, angles, and ratios. Because of this dependence on CMA, most discriminators used for sexing, although not all, were primarily based on size. However, sexual dimorphism in human skeletons is not just a matter of size. Shape differences are also very conspicuous, e.g., in the human hip bone (9). It is therefore important for sex determination studies to examine not only size differences of the human skeletons, but also shape differences. In order to properly appreciate and measure the shape differences, it is necessary to first eliminate the size factor, and this has usually been done by constructing indices based on linear measurements. Unfortunately, such indices do not adequately provide for separation of the contributions that size and shape make to the overall skeletal morphology. Thus, indices are not only inadequate measures for the control of size differences, but also mask the problems of shape definition and shape change (10–12).

Boundary morphometrics, such as Fourier descriptors, can be considered as an innovative improvement compared to CMA. Fourier analysis provides a much more accurate and useful quantitative description of the irregular boundary of biological forms. This method allows correction for size differences as well as providing separation of the contributions that size and shape make toward the global morphology. Conventional Fourier descriptors have been used for quantitatively analyzing sex differences in shape of two-dimensional outlines, e.g., the forehead shape of skull (13) and soft tissue facial shape (14). The use of conventional Fourier analysis, however, contains constraints because of: (1) the use of equal divisions over the interval or period, (2) the restriction to simple classes of morphological forms, and (3) the presence of outlines that curve back on themselves (10,15,16). A newer formulation, elliptical Fourier functions (EFFs), derived as a parametric formulation from conventional Fourier analysis, circumvents these problems (10,17). Previous studies have demonstrated that the EFF approach is a particularly efficient method for numerically describing the form of complex morphological two-dimensional outlines (18–21). Thus, it should be possible to produce more accurate sex determinations with a quantitative analysis based on EFFs.

Furthermore, using a multivariate approach, accuracy rates in

[1] Laboratory of Human Ergology, Department of Human-Computer Interaction Science, Tokyo University of Agriculture and Technology, Japan.

[2] Section of Oral Biology, School of Dentistry, University of California at Los Angeles, Los Angeles, CA.

[3] Laboratory of Health and Amenity Sciences, Department of Eco-design, Tokyo University of Agriculture and Technology, Japan.

[4] Department of Anatomy, The Jikei University School of Medicine, Japan.

[5] Department of Human Morphology, Graduate School of Science, Tokyo Metropolitan University, Japan.

Received 20 Oct. 1998; and in revised form 22 Jan. 1999, 7 June 1999; accepted 2 July 1999.

the quantitative determination of sex should increase if based on measurements from as many skeletal elements as possible. On the other hand, it would be also beneficial if one could identify what area within a single bone would yield the most accurate determination of sex. Recently, sex determinations based on a single bone have focused on long bones such as the femur and tibia, since those are subjected to heavy stress during an individual's life and that stress may have a sexual component (5,6). Another study of sex determination used the humerus. The humerus was chosen because it is not a weight-bearing long bone and presumably less affected by differences in size, and therefore possibly reflecting sex differences (22). This study also proposed the necessity of osteometry at muscle origin and insertion in sex determinations and suggested that measurements of the proximal humerus are exceptionally accurate in predicting sex rather than those of the distal humerus. Nevertheless, few studies have used the proximal humerus for this purpose. The primary focus of the present study is to numerically examine the human proximal humeral outline for possible sex differences in size and shape using EFFs. In addition, the proximal humeri will also be analyzed with discriminant functions in an effort to test the accuracy of these sex determinations.

Methods

Materials

Right and left humeri pairs of 69 individuals, 36 males and 33 females, were selected from a skeletal collection available at the Department of Anatomy, the Tokyo Jikei University School of Medicine. These subjects represent adult Japanese who were born between 1856 and 1921. Means and standard deviations of the age at death were 38.1 ± 12.2 years old for males and 34.3 ± 11.4 years old for females, respectively. These data were obtained from cadaver records, in which the sex, date of birth, birthplace, cause of death, and date of death were documented for each specimen. The skeletal samples were carefully chosen according to the following criteria: (1) possession of intact and complete left and right humeri, (2) absence of any gross pathological changes in skeletal structure, and (3) preservation of critical areas identifying the origin and insertion of muscles.

Photographs

Photographs were taken of the superior view of the proximal humeri. Each bone was rigidly oriented on a specially designed humeral holder. This holder was designed to locate the bone reference axes as precisely and consistently as possible in order to eliminate bone-positioning errors. Details of the humeral holder and the photographic method are available from a previous study (21). Briefly, the orientation of the three standardized planes for each bone was carried out with the following procedure. Each humerus was placed dorsal side down, on the flat surface of the humeral holder. The sagittal plane of the humerus is defined by the mediolateral midpoints of two locations on the shaft, which are approximately located on the distal- and proximal-quartile points to the humeral length. The frontal plane is defined as a plane parallel to the flat surface, passing through the center of the capitulum humerus, and perpendicular to the sagittal plane. The longitudinal axis of the diaphysis is formed by the intersection of these two planes. The same procedure for bone orientation and the reference axes was applied to all specimens.

The height of the longitudinal axis for each bone was measured parallel to the floor with a ruler. A 35-mm camera (Nikon F90x) with an extension tube (Nikon PK-13) and an 800 mm telephoto lens (Tokina T 800 mm F8.0) was positioned so that the height of its optical axis from the floor was equal to that of the longitudinal axis. The distance between object and camera was 13.5 m, a length necessary to maintain the measurement distortion to less than 1% (23). Black and white photographic prints were enlarged (1:1) to the original size of humerus. Using a light table, dimensionally stable acetate film was placed on top of each photograph and each proximal humeral outline was carefully traced with a 0.3-mm lead mechanical pencil.

Digitization

Fifty-four points were constructed along the outline of the proximal humerus in the following manner. Reference should be made to Fig. 1 for location of points identified below within brackets. Initially, two points on the edges of the greater tubercle [1] and of the lesser tubercle [17] to the humeral head were marked on the outline tracing and defined as anatomically homologous points. A dashed line was then drawn as a tangent to the outer margins of both edges of the intertubercular groove (ITG). Subsequently, a parallel dashed line was drawn through the deepest aspect of the ITG concavity. These tangent points were defined as points [26], [36], and [31], respectively. The line from point [1] to point [17] was bisected at point [O] and the intersection of the perpendicular with the proximal humeral outline generated point [9]. A perpendicular through the mid-point of the line from point [36] to [1] generated point [46]. Lines L1 to L7 were drawn connecting these points.

The distances of L1, L2, L3, L6, and L7 lines were divided into eight equal subdivisions and the L4 and L5 lines were similarly bisected into five subdivisions. Perpendicular lines from the bisections of L1–L7 were then extended to the proximal humeral outline defining points 2–8, 10–16, 18–24, 27–30, 32–35, 39–45, and 47–53, respectively. Points [25] and [54] are additional bisections. Points [37] and [38] are trisections between points [36] and [39]. These latter four points were added because the EFF program, subsequently utilized, required that the number of points entered to be a multiple of six. This happens to be constraint of the software.

Once the 54 points were located on the proximal humeral outline, the data were submitted to a software program EFF23, DOS version 2.6 (24) that controlled the (1) digitizing, (2) plotting, and (3) computation of EFF coefficients and bounded areas of the outlines.

The proximal humeral tracing was digitized using a Graphtec KD4320 digitizer with an accuracy of approximately 0.1 mm. A so-called "mirror image" of the left humeral tracing was constructed by reversing the semitransparent acetate film. The mirror imaging was carried out to orient the right and left sides so that their outline tracings are in the same orientation. Each humeral tracing was then placed on the digitizer with the point [O] superimposed on the center of digitizer pad (0,0) and the line from point [O] to [9] made coincident with a reference line drawn at a 35-deg angle to the horizontal axis of the digitizer crosshairs. This was done to ensure an initially constant orientation.

All points from point [1] to [54] were digitized in a clockwise order and entered as data to the EFF program on an IBM compatible PC. The digitized points were subsequently plotted using a Hewlett-Packard laser jet printer and superimposed on the originally traced points to check for digitizing errors for each specimen. Excellent replicability of the digitization procedure has been already demonstrated in an earlier study (21).

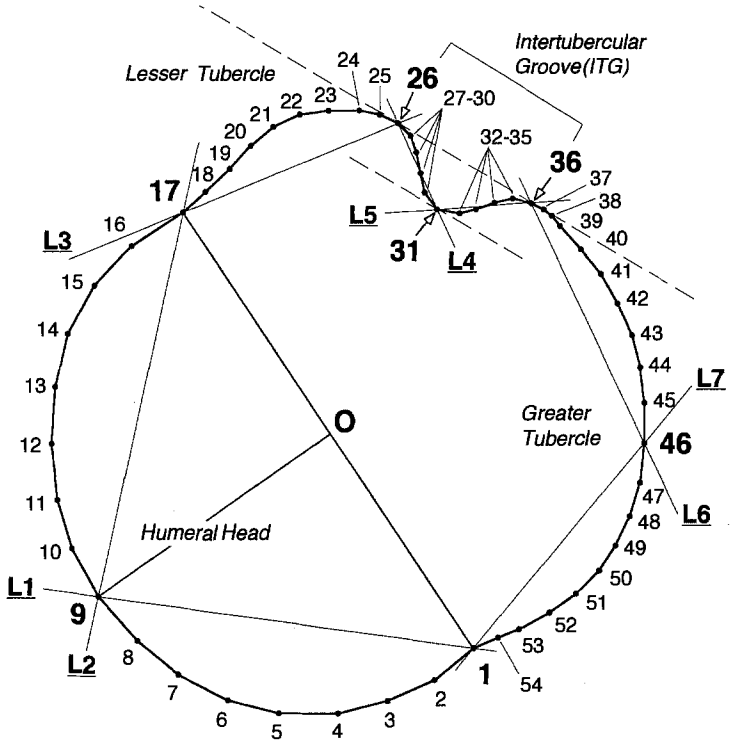

FIG. 1—*Schematic diagram of the 54 points used to characterize the proximal humeral outline. The dashed line is a tangent line through the outermost margin (points 26 and 36) on both edges of the intertubercular groove (ITG). The other dashed line parallel to it, was constructed at the deepest aspect (point 31) of the ITG concavity. The lines L1 to L7 were used to develop the geometry required to locate the 54-point system.*

Elliptical Fourier Functions (EFFs)

The proximal humeral outline was numerically described with elliptical Fourier functions as wave forms based on the observed data points. The elliptical Fourier descriptor is based on an orthogonal decomposition of a curve into a sum of harmonically related ellipses. This decomposition is parametric. That is, both x and y coordinates are defined as functions of time, or t. The advantage of the elliptical Fourier decomposition is that segment lengths can now vary along a polygon, and since the *changes in x- and y-directions are treated independently,* the curve can take any shape and even have self-intersections (17). If a point travels along the polygon, representing the outline, at constant speed, then the x-coordinate can be separately defined as a function $x(t)$ on time t. This function is single-valued, piecewise linear, continuous, and periodic (as the point travels repeatedly around the closed curve). This function has a Fourier expansion of sine and cosine terms, which comprise a curve of integer frequencies with their associated amplitudes. An identical decomposition is possible with the y-coordinate $y(t)$ of the polygon. Since the EFF is parametric, one can separate the x- and y-axis contributions as projections onto their respective axes. The x-y representation of an original outline and its x and y projections are shown in Fig. 2.

For all positive integers n, there is a trigonometric curve (the sum of the sine and cosine terms) representing the nth harmonic of the x- or y-projection of the polygon. Giardina and Kuhl have demonstrated that for any particular n, when these two curves are joined in the parametric formulation, they define an ellipse in the x-y-plane (25). To reconstruct the original polygon, these ellipses are vector-added together for all harmonics. The reconstruction from k harmonics is a best-fit in a least-squares sense. In other words, the integral along the polygon of the squared (x- or y-direction) differences between the polygon and the partial sum for k terms of a trigonometric series is a minimum when the coefficients for the series are the Fourier coefficients.

The parametric equations are defined such that the Fourier series in $x(t)$ is given as

$$x_p = f(t) = A_0 + \sum_{n=1}^{k} a_n \cos(nt) + \sum_{n=1}^{k} b_n \sin(nt) \qquad (1)$$

and the Fourier series in $y(t)$ as

$$y_p = f(t) = C_0 + \sum_{n=1}^{k} c_n \cos(nt) + \sum_{n=1}^{k} d_n \sin(nt) \qquad (2)$$

where A_0 and C_0 are constants, a_n, b_n, c_n, and d_n are the Fourier coefficients, n equals the harmonic number, k equals the maximum harmonic number, and the period is defined over a 2π interval.

For the samples of the present study, the EFFs were truncated at 27 harmonics, which is one-half the number of digitized points because of Nyquist frequency restrictions. The goodness-of-fit of the EFF with 27 harmonics for each outline was checked by calculating the mean residual averaged over the 54 points. This mean residual is the mean difference between the expected points, derived from the EFF, and the original observed points on the outline. Mean and standard deviation values for the mean residual, based on the total database (n = 138, i.e., 69 pairs of humeri), were 0.070 ± 0.010 mm. This value is considerably less than the errors associated with both the tracing and digitizing procedures. Twenty-seven harmonics require a matrix of 108 separate terms, four coefficients (a_n, b_n, c_n and d_n) for each harmonic and two constants (A_0 and C_0) for each function. Background and derivations of the constants and coefficients in Eqs 1 and 2 can be found in Kuhl and Giardina (17) and Lestrel (16).

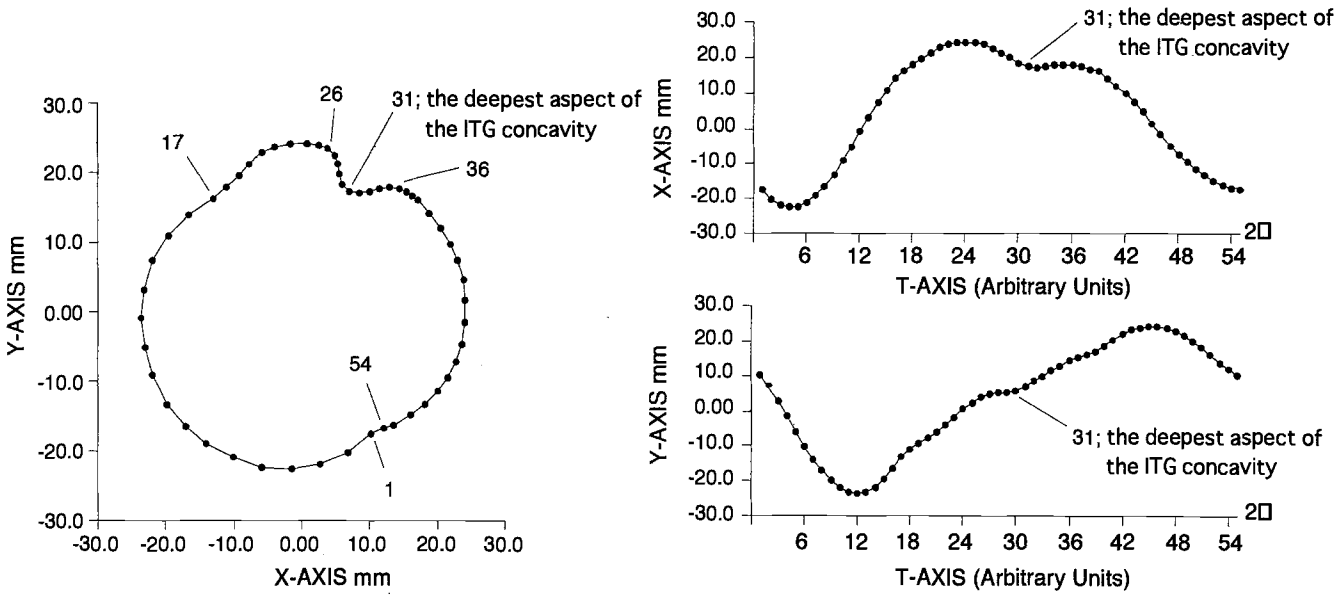

FIG. 2—*Cartesian coordinate plots* (x, y), (t, x), *and* (t, y) *of the proximal humeral outline. Left graph is an original presentation. Right upper graph shows the* x*-coordinate values (*x *projections) plotted as a function of a third variable,* t, *on the horizontal axis. Right lower graph displays the* y*-coordinate values (*y *projections) plotted as a function of a third variable,* t, *on the horizontal axis.*

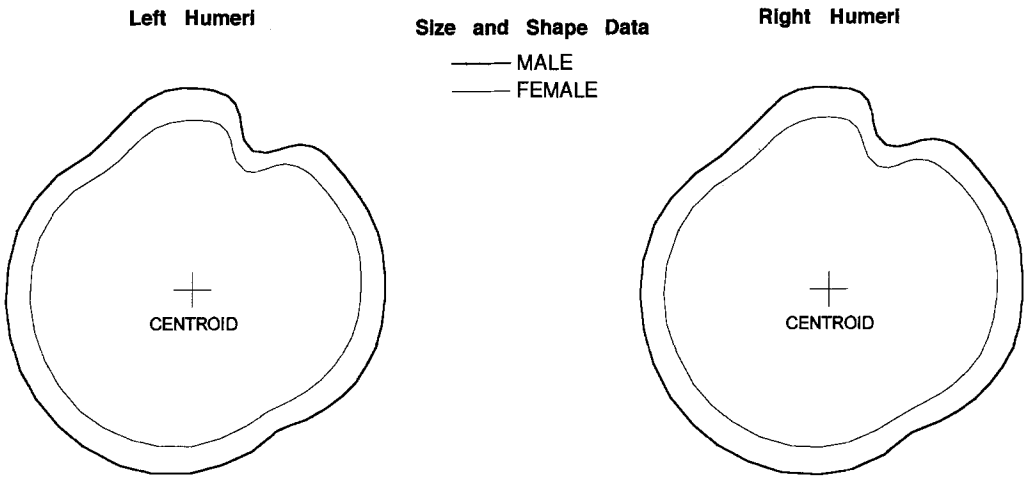

FIG. 3—*Mean plots of the male and female humeral outlines for each side. These data were superimposed on the centroid. The left humeral outlines are presented as a mirror image.*

Once the EFF coefficients were computed, they were used to calculate amplitudes, the variance (or power spectrum), and the percent of the variance explained. These were computed separately for the x and y directions for each outline. The amplitude, or height of the wave, is the square root of the sum of the squared coefficients preceding the cosine and sine terms for each harmonic. The variance of each harmonic is equal to the squared amplitude divided by two. The total variance is the summation of all variance values. Thus, the percentage variance explained in terms of the total variance represents relative magnitude (or contribution) of the amplitude for each harmonic and hence indicates characteristics of the complex outline forms as a whole.

Results

Figure 3 displays the mean male data superimposed on the mean female data using the centroid for each side. In the figures presented here, the right-left directions as viewed from the centroid, represent lateral-medial directions on the humerus, while the upward-downward directions represent anterior-posterior, respectively. The mean outlines for the female humeri lie within the male outlines for both the right and left sides. The magnitude of sex differences in size and shape of the proximal humeral outlines were quite large, mainly due to differences in size.

The bounded areas of the proximal humeral outline were computed using EFFs based on the "size and shape" data (i.e., not size-standardized EFFs), representing the transverse aspect of the proximal humerus. The maximum humeral length (26) was measured directly from the skeletal material, representing longitudinal size of the humerus. These two variables, humeral area and length, were analyzed simultaneously using a one-way MANOVA separately for each side of the humerus. The bounded area and the maximum length showed statistically significant sex differences; Wilk's lambda = 0.32 for the both sides, $P < 0.01$ (Table 1). Univariate

F-tests showed statistically significant sex differences in the maximum length. Male humeri were significantly longer than female humeri on the right side (10.1%, F (1, 67) = 51.1, $P < 0.01$) and the left side (10.6%, F (1, 67) = 54.9, $P < 0.01$). Statistically significant sex differences in the bounded area were also detected with the univariate F-tests. Male humeri were pronouncedly larger in bounded area than the female humeri, both on the right (34.7%, F (1, 67) = 143.4, $P < 0.01$) and left sides (34.9%, F (1, 67) = 144.4, $P < 0.01$). These results indicated that sex differences of the humeral length and especially the transverse area (as a measure of size) of the proximal humeri were pronounced for both sides. Moreover, these statistically significant sex differences in proximal humeral outline size can be visually assessed from the mean outline plots (Fig. 3).

Figure 4 displays the size-standardized mean data with females superimposed on the male data using the centroid. Each side is shown separately as a way of visually displaying the sex differences in shape of the proximal humeral outlines. In the present study, size standardization was accomplished by scaling all bounded outlines, so that the area within each specimen was equal to 10 000 mm^2. After size standardization, the mean male outlines showed a close correspondence to the female right and left outlines (compare with Fig. 3). We focus now on the more localized regional differences. The greater tubercle (points 36–1) was located more postero-medially and the lesser tubercle (points 17–26) was located more anteriorly in the males compared to females. This is indicated with the solid arrows in Fig. 4. Amplitudes versus harmonic number plots were then used to establish whether the displayed differences were statistically significant.

Figures 5 and 6 illustrate amplitude versus harmonic number plots for the right and left humeral outlines, respectively. The vertical scale in these plots has been magnified to display the variability in the higher harmonics. These amplitudes are derived from the "size-standardized" EFFs, and the mean data for each sex group are plotted along the ordinate. The 27 amplitudes were analyzed simultaneously using a one-way MANOVA, independently for the x- and y-directions. The amplitudes on the right side humeri showed statistically significant sex differences for both the x- and y-directions (Wilk's lambda = 0.32 for the x-direction, $P < 0.01$; and 0.41 for the y-direction, $P < 0.05$). For the left side humeri, statistically significant sex differences were also detected (Wilk's lambda = 0.45 and 0.41 for both the x- and y-directions, respectively, $P < 0.05$). Univariate F-tests showed statistically significant sex differences for many of the specific harmonics, as indicated with the arrows in Figs. 5 and 6. The number of harmonics with significant values was larger for the right humeral data than for the left humeral data, especially in the x-direction. Table 2 shows means and standard deviations of the first harmonic amplitude for the x- and y-directions, excluding the higher harmonics. The amplitude of the first harmonic also showed significant sex differences in the x- and y-directions for the both sides of the humeri.

The predicted EFF curve fit with 27 harmonics was a very close analog of the observed data points on the proximal humeral outlines, as already mentioned. Of the 27 harmonics, the highest percentage contribution in terms of the total variance was the first harmonic. Calculations of the mean percentage of the variance explained by the first harmonic were carried out separately for the male and female samples, and sex differences were tested using a one-way ANOVA. No significant sex differences were found for both the x- and y-directions, allowing for the pooling of this data. The mean values of the first harmonic percentage explained were 99.5% with respect to the total variance, based on total database for both the x- and y-directions. The reason for such a high percentage

TABLE 1—*Means, standard deviations, and univariate* F-*ratios for the maximum length and bounded area for each side of the humerus.*

	Males (n = 36)		Females (n = 33)		
	Mean	S.D.	Mean	S.D.	F-ratio‡
		RIGHT			
Maximum length*	297.1	17.62	269.8	13.60	51.11**
Bounded area†	1651.5	187.79	1226.4	82.76	143.40**
		LEFT			
Maximum length	294.6	17.67	266.4	13.57	54.86**
Bounded area	1622.0	184.87	1201.9	81.75	144.40**

* Direct measurements (mm).
† Bounded area of the proximal humeral outline (mm^2).
‡ Statistical significance was determined from the univariate F-test within each side of the humerus associated with a one-way MANOVA (**$P < 0.01$).

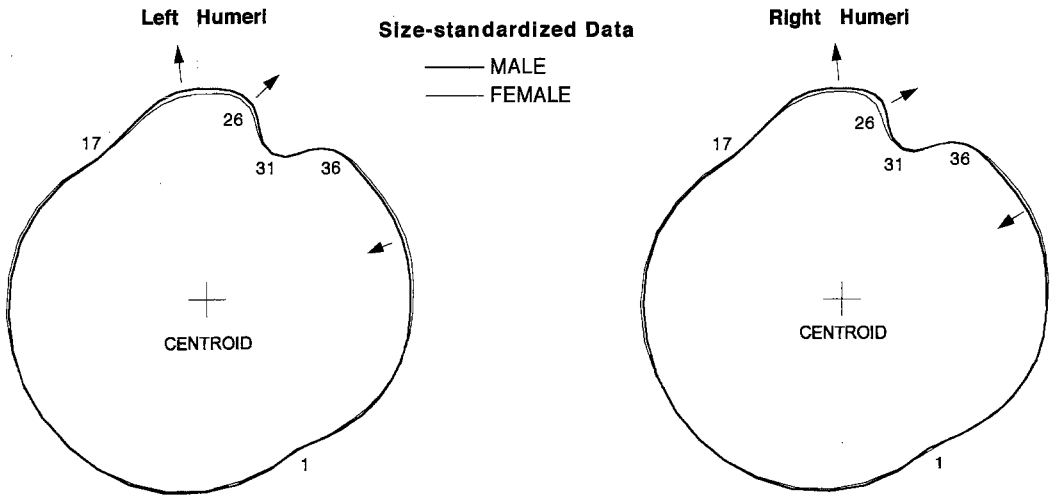

FIG. 4—*Mean plots of the male and female humeral outlines for each side. These data were area-standardized and superimposed on the centroid. The left humeral outlines are presented as a mirror image. Solid arrows indicate the major sex differences in outline shape as viewed from female to male data.*

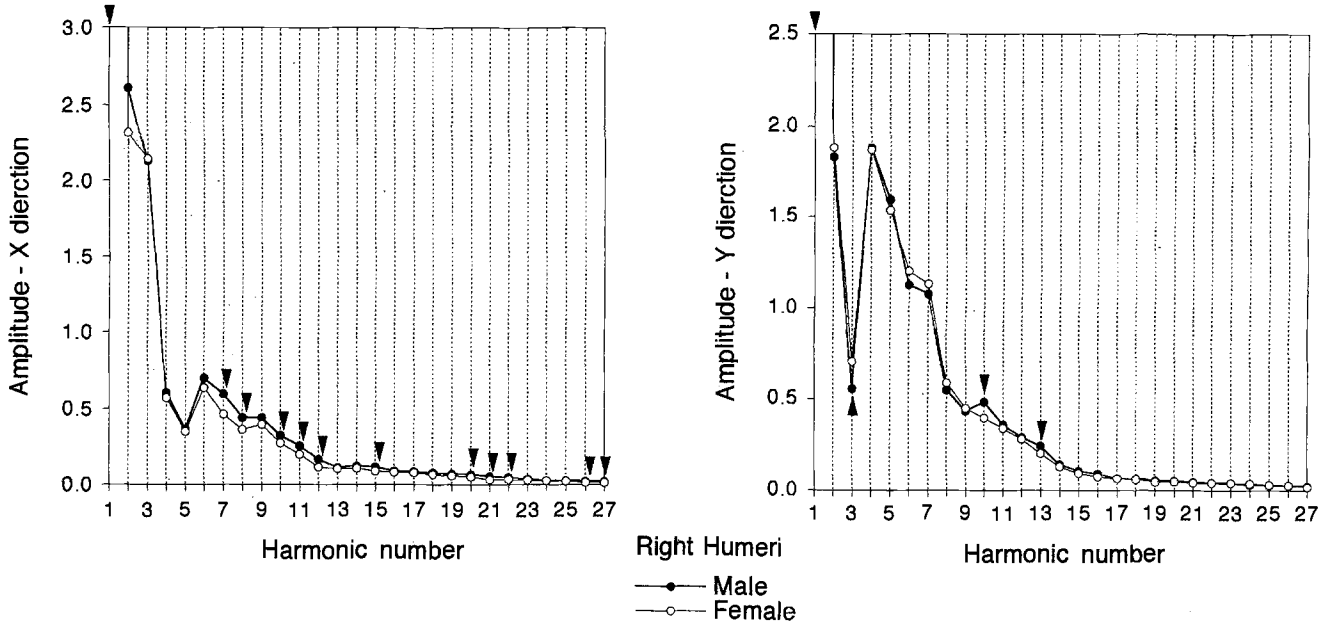

FIG. 5—*Amplitude vs. harmonic number plot of the right humeral outline for pooled male and female samples. Amplitude plots were magnified to display the variability in the higher harmonics. Solid arrows indicate statistical significant sex differences* ($P < 0.05$).

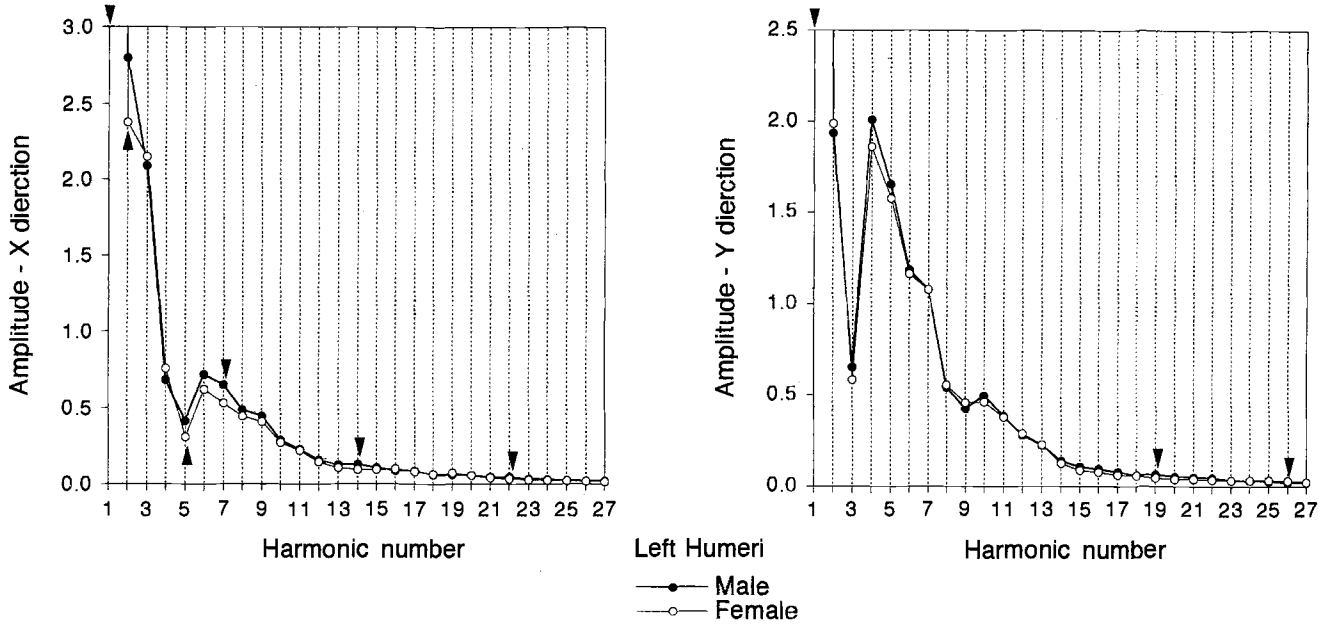

FIG. 6—*Amplitude vs. harmonic number plot of the left humeral outline for pooled male and female samples. Amplitude plots were magnified to display the variability in the higher harmonics. Solid arrows indicate statistical significant sex differences* ($P < 0.05$).

is that the shape of the proximal humeral outline is rather elliptical to begin with. Thus, the first ellipse, i.e., the predicted EFF curve fit with one harmonic, can be used as a reasonable description of the proximal humeral outline shape as a whole. It can be shown that the EFF amplitudes for the first harmonic are related to the semi-major and semi-minor diameters of the first ellipse. Accordingly, the ratio of the major axis divided by the minor axis was computed and then averaged separately for right and left humeri (Table 3). Statistically significant sex differences were found for both right and left sides. Female humeri showed significantly larger mean values of the ratio than the male humeri.

If the above results are an accurate reflection of the sexual differences, then these measures (amplitudes) should be good discriminators of sex. One way to test this hypothesis is to compute discriminant functions and look at the misclassification rate. All of the 54 amplitudes (i.e., 27 harmonics × 2 directions) derived from the "size-standardized" EFFs were entered as independent variables into a stepwise discriminant function analysis. These variables represented shape characteristics of the proximal humeral outline. Tables 4 and 5 show the standardized coefficients of the discriminant functions for the right and left humeri, respectively. The number of the variables kept in the stepwise solution was

TABLE 2—*Means, standard deviations and univariate F-ratios for the first harmonic amplitudes for each side of the humerus.*

	Males (n = 36)		Females (n = 33)		
	Mean	S.D.	Mean	S.D.	F-ratio*
		RIGHT			
x-direction	56.95	0.62	57.60	0.57	20.60**
y-direction	55.51	0.57	54.87	0.52	23.72**
		LEFT			
x-direction	56.78	0.62	57.51	0.57	25.73**
y-direction	55.63	0.61	54.93	0.56	23.97**

* Statistical significance was determined from the univariate F-test within each side of the humerus associated with a one-way MANOVA, independently for the x- and y-directions (**$P < 0.01$).

TABLE 3—*Mean ratios of the major axis divided by the minor axis in the predicted EFF curve fit with one harmonic: sex differences in global shape of the proximal humeral outline.*

	Male		Female		
	Mean	S.D.	Mean	S.D.	F-ratio†
Right	1.057	0.025	1.072	0.028	5.39*
Left	1.054	0.023	1.071	0.024	9.10**

† Statistical significance was determined with a one-way ANOVA, separately for each side of the humerus (*$P < 0.05$, ** $P < 0.01$).

TABLE 4—*Standardized canonical discriminant function coefficients for computing an individual discriminant function score from amplitudes of the size-standardized EFFs for right humeri.*

Harmonic No.	Coeff.	Harmonic No.	Coeff.
X 1	10.15	Y 1	9.94
X 2	0.78	Y 2	...
X 3	...	Y 3	...
X 4	...	Y 4	...
X 5	0.48	Y 5	...
X 6	...	Y 6	0.52
X 7	1.60	Y 7	...
X 8	...	Y 8	...
X 9	0.56	Y 9	0.98
X 10	...	Y 10	0.76
X 11	...	Y 11	...
X 12	0.68	Y 12	−0.56
X 13	−0.35	Y 13	1.01
X 14	−0.29	Y 14	...
X 15	...	Y 15	0.46
X 16	...	Y 16	...
X 17	−0.76	Y 17	...
X 18	...	Y 18	...
X 19	...	Y 19	...
X 20	...	Y 20	−0.30
X 21	0.41	Y 21	0.30
X 22	−0.39	Y 22	...
X 23	...	Y 23	...
X 24	...	Y 24	−0.52
X 25	...	Y 25	−0.57
X 26	1.09	Y 26	...
X 27	0.87	Y 27	...

TABLE 5—*Standardized canonical discriminant function coefficients for computing an individual's discriminant function score from amplitudes of the size-standardized EFFs for left humeri.*

Harmonic No.	Coeff.	Harmonic No.	Coeff.
X 1	−1.86	Y 1	...
X 2	−3.88	Y 2	...
X 3	1.99	Y 3	0.26
X 4	−1.54	Y 4	...
X 5	...	Y 5	−3.97
X 6	1.23	Y 6	1.63
X 7	4.47	Y 7	1.98
X 8	1.79	Y 8	...
X 9	−0.99	Y 9	...
X 10	1.20	Y 10	...
X 11	0.80	Y 11	0.95
X 12	−1.05	Y 12	−1.93
X 13	...	Y 13	−2.18
X 14	...	Y 14	0.77
X 15	...	Y 15	0.47
X 16	−1.45	Y 16	...
X 17	1.22	Y 17	−0.38
X 18	−1.20	Y 18	...
X 19	...	Y 19	1.11
X 20	−0.66	Y 20	0.46
X 21	...	Y 21	...
X 22	...	Y 22	0.68
X 23	0.65	Y 23	1.12
X 24	...	Y 24	0.88
X 25	...	Y 25	...
X 26	0.47	Y 26	−1.00
X 27	...	Y 27	...

larger for the left side when compared with the right. These results suggest that the sexual dimorphism in shape of the proximal humeri for the left side is somewhat different from the right side.

The bounded area of the proximal humeral outline and the maximum humeral length, as size measurements, were simultaneously entered into the stepwise discriminant function analysis. These were run separately from the amplitude data mentioned above. The bounded area was kept while the maximum length was removed from the stepwise solution. Discriminant scores were independently calculated from these discriminant functions based on the bounded area and the amplitudes derived from the size-standardized EFFs, and then plotted in Cartesian two-dimensional space. The two-dimensional plots were used to simultaneously display results of sex discrimination expected with each function. When the score is smaller than zero, the judgment is feminine. When it is larger than zero, the judgment is masculine. Figures 7 and 8 display this two-dimensional distribution of the discriminant function scores for the right and left humeral data, respectively. Open circles indicate individual females and solid circles show individual males. For the right humeri, three male cases were classified into the feminine group with the bounded area function, but those three were correctly assigned into the masculine group with the amplitudes function (as indicated with open arrows). Conversely, all of the female cases were correctly classified into the feminine group with the bounded area, but one female case was misclassified with the amplitudes as masculine (as indicated with a solid arrow). For the left humeri, five male cases that were classified into the feminine group with the bounded area, but were correctly assigned to the masculine group with the amplitudes. All of the female cases were classified into the true group as feminine with not only the bounded area, but also with the amplitudes. With respect to classi-

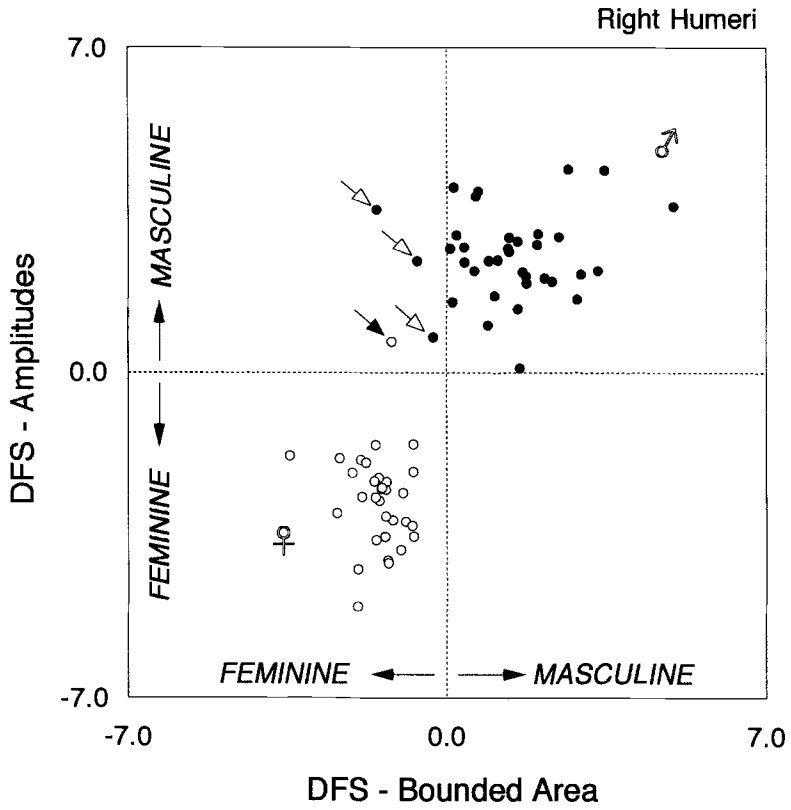

FIG. 7—*Two-dimensional distribution of discriminant function scores for the right humeral data. The discriminant scores (DFSs) based on the bounded area and the Fourier amplitudes derived from the size-standardized EFFs are plotted along the abscissa and ordinate, respectively.*

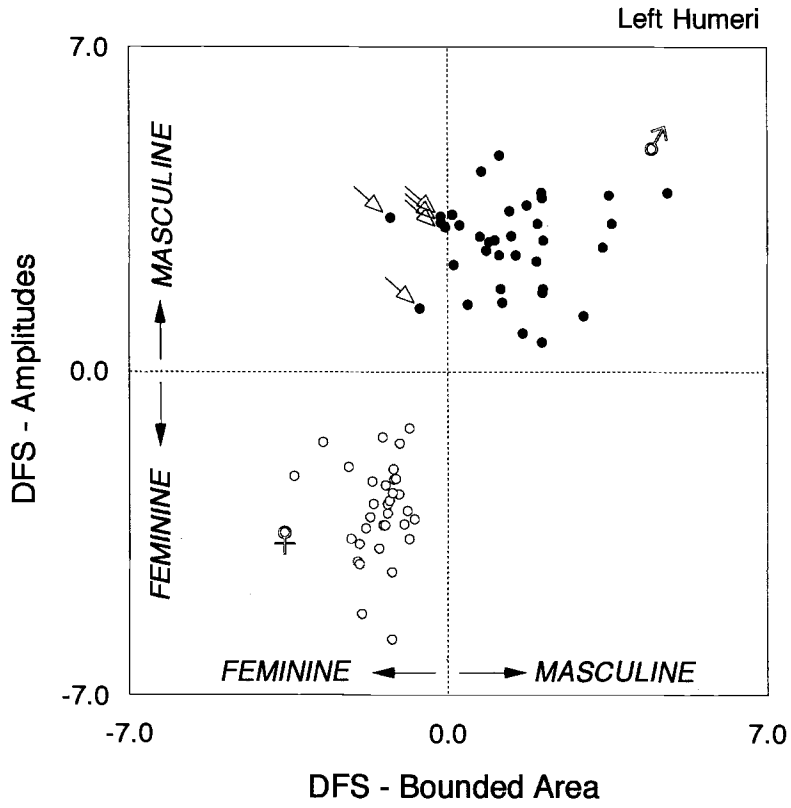

FIG. 8—*Two-dimensional distribution of discriminant function scores for the left humeral data. The discriminant scores (DFSs) based on the bounded area and the Fourier amplitudes derived from the size-standardized EFFs are plotted along the abscissa and ordinate, respectively.*

TABLE 6—*Percentage of cases correctly assigned within each group.*

Functions	Methods§	Total *n*	Males %	Males *n*	Female %	Female *n*	Average %
			RIGHT				
Bounded area*	*Original*	69	91.7	33/36	100.0	33/33	95.7
	CV		91.7	33/36	100.0	33/33	95.7
Amplitude†	*Original*	69	100.0	36/36	97.0	32/33	98.6
	CV		88.9	32/36	97.0	32/33	92.8
			LEFT				
Bounded area*	*Original*	69	86.1	31/36	100.0	33/33	92.8
	CV		86.1	31/36	100.0	33/33	92.8
Amplitude‡	*Original*	69	100.0	36/36	100.0	33/33	100.0
	CV		94.4	34/36	90.9	30/33	92.8

* Discriminant function based on the bounded area of the proximal humeral outline.
† Discriminant function based on the amplitudes derived from the size-standardized EFFs, as shown in Table 4.
‡ Discriminant function based on the amplitudes derived from the size-standardized EFFs, as shown in Table 5.
§ The classification percentages were calculated with an ordinary method using the original samples (Original) and a cross-validation method (CV), respectively.

fication based on the original database, the average percentages of cases correctly classified for the right humeri were 95.7% for the bounded area function and 98.6% for the amplitudes function, respectively. The average percentages for the left humeri were 92.8% for the bounded area and 100.0% for the amplitudes, respectively (Table 6).

In order to determine whether sample related factors contribute to these results the samples were classified again using a cross-validation method. The statistical software program used was DISCRIMINANT from the SPSS package for the Windows95 release 7.5 (Japanese version). As shown in Table 6, mean values of the average percentages showed also a high rate of correct classification under cross-validation. It should be noted that using the amplitudes function, the average percentages of correct classification decreased from 98.6% to 92.8% for the right humeri and from 100% to 92.8% for the left humeri. However, the remaining high rate of correct classification under cross-validation indicates that the sampling error was generally less. These results strongly suggested that the EFF parameters, such as the bounded area and amplitudes, are useful for sex determinations based on discriminant function analyses.

Discussion

In the present samples, significant sex differences in absolute size of the proximal humeri evidently existed for both the right and left sides. That is, males were much larger in the bounded area of the proximal humeral outline than females. The maximum humeral length also showed significant sex differences, but this measurement was removed from the stepwise discriminant function. This suggests that the transverse size measurement of the proximal humeri can be a useful discriminator for sexing rather than the more usual longitudinal size measurement. Past sex-determination studies of long limb bones demonstrated that cross-sectional or transverse dimensions such as the diameter of the femur head or the epicondylar width of the humerus were actually more accurate discriminators than longitudinal dimensions such as humeral and femur lengths (1,8,27,28). However, France has further discussed this problem and suggested that any study of bone should include a consideration of the areas of muscle attachment because of their relationship to sexual dimorphism (22). This implies that a "newer" morphometrics needs to be developed for a more accurate determination of sex differences, including aspects of size and shape at areas of muscle origin and insertion instead of the "older" morphometrics depending solely on CMA.

If size differences are at all appreciable, as the case of the present study, subtle shape differences may be confounded and possibly overwhelmed by the effect of size. After size-standardization, we can theoretically examine the subtle shape differences under minimizing the effect of size factor. Using the EFF approach, size-standardization was accomplished by scaling all bounded outlines to a constant area. Once size has been controlled, differences in outline shape can be depicted visually and analyzed statistically. The sex differences in shape of the greater and lesser tubercular regions, while subtle, were noticeable in the current study (Fig. 4). Interestingly, the lesser tubercle of male humeri was relatively protruded with respect to the female one, while the greater tubercle showed a contrasting pattern. These shape differences indicate that the tubercular aspects of the male humeri are medio-laterally expanded compared to the female humeri.

The amplitudes calculated from the "size-standardized" EFFs, showed statistically significant sex differences (Figs. 5 and 6). For the EFFs, the separate harmonics produce ellipses. These ellipses when summed will converge onto the polygon that serves as the original form. Thus, differences in the EFF coefficients (and their associated amplitudes) can be interpreted in an analogous fashion to conventional Fourier coefficients. That is, the first few harmonics describe global differences in shape and the higher harmonics describe more localized aspects (12,16,18). Armed with this information, the amplitude differences in the first harmonic (separately for the *x*- and *y*-directions) can be evaluated. They seem to reflect the sex differences seen in the global shape of the proximal humeral outline. The amplitude of the first harmonic showed significant sex differences in the *x*- and *y*-directions for both sides of the humeri. In addition, sex differences in the ratio of the major/minor diameters were analyzed for the first harmonic, numerically representing sex differences in shape of the first ellipse. Female humeri showed significantly larger mean values of the ratio than male humeri for the right and left sides (Table 3). When the ratio is equal to 1.0, the ellipse shape becomes a true circle. These results therefore indicated that the cross-sectional outline of the human proximal humeri is quite circular in global shape. Interestingly, both right and left proximal humeri appear to be more circular in males when compared to that in females. In other words, the fe-

males display a slightly more elliptical than circular global shape in contrast to males. Careful scrutiny of Fig. 4 shows that this, indeed, is the case. These results strengthen the contention that sexual dimorphism in global shape of the proximal humeral outlines exists.

General observations from gross anatomy indicate that the greater and lesser tubercles provide areas for the insertion of the rotator cuff muscles. The two tubercles are separated from each other by a deep groove, the ITG, which houses the tendon of the long head of the biceps brachii muscle. The rotator cuff muscles and the tendon of the long head have been identified as one of the dynamic stabilizers of the glenohumeral joint (29–32). Surfaces of the tubercular regions, including the ITG, will always be subjected to, in vivo, tensile stresses generated from these muscular contractions. It is assumed that the differences in these tubercular areas of the proximal humerus (as muscular insertions) are primarily due to being subjected to forces. These forces, in turn, are leading to the addition of more bone by the piezoelectric effect. The effects of such muscle pulls will be significantly more related to environmental factors than to genetic ones. Thus, the sex differences in outline shape of the tubercular areas of the proximal humerus (but not in size) found here, may be largely attributed to environmental factors. These are assumed to be due to activity differences between males and females, possibly, in part, dependent on culturally prescribed sex roles.

Cross-cultural investigations have demonstrated that populations with different economic activities had different relative sexual dimorphism levels (33,34). Thus, it is postulated that the measurements around areas of muscle insertion should not be applied cross-culturally in sex determination studies, especially where occupational differences are obvious (22). In the present study, the humeral specimens consisted of Japanese males and females who were born from 1856 to 1921 and died from 1925 to 1952. That is, most lived before World War II ($n = 60$) and a few during WW II ($n = 9$) in Tokyo. It can be thought that their nutritional conditions were better than after WW II. The females, on the other hand, who had no occupation outside of the home (i.e., "homemakers") accounted for 87.9% ($n = 29/33$) of all females, while almost all the males worked. Most males and females having occupations outside of the home consisted of diverse industrial workers such as factory hands and electricians, or "handy craftsmen," but did not include any agricultural workers in the country. Sexual division of labor was, perhaps, more pronounced in Japan then, than in recent times. Thus, it could be expected that these socio-culturally prescribed sex roles influenced the sexual dimorphism in size and shape of the proximal humeri observed here.

Since the Fourier coefficients reflect the property of orthogonality, they can be further analyzed separately with conventional statistics. The sex of the present samples was quantitatively described with two types of discriminant function scores. These were estimated with (1) size variable such as the bounded area of outlines, and (2) shape variables such as the amplitudes derived from the "size-standardized" EFFs. The discriminant functions constructed with the size and shape variables were sufficient in providing for an accurate sex determination approaching 100% within the present population. This high value may be the result of the homogeneity of the Japanese population with respect to race and socio-cultural background. However, the present results strongly suggest that the EFF method (e.g., the use of amplitudes derived from EFFs) is useful for numerically analyzing sex differences in size and shape of two-dimensional outlines.

Finally, a number of limitations with this study needs to be mentioned: (1) the sample sizes are too small to adequately serve as norms, (2) accuracy of the sex determinations has not been tested on other samples, and (3) the analysis is restricted to two dimensions, e.g., superior view of the humerus. Nevertheless, such outline form studies should be continued in other populations of the same and different races. Finally, by extending such methods to three dimensions, the numerical analysis of the proximal humeral morphology may provide one of the more useful discriminators for studying sexual dimorphism in humans.

Conclusions

The EFF approach (i.e., "boundary morphometrics" focusing on the outline of forms) revealed that sexual dimorphism in transversal size and shape of the human proximal humeri exists in a modern Japanese population. The measurements derived from EFFs seem to be sufficient for accurate sex determinations. Moreover, the use of discriminant functions analysis, in conjunction with the data derived from EFFs, succeeded in obtaining higher accuracy levels for sexing compared with previous studies based on CMA.

The present study has demonstrated that the size and shape of the proximal humeral outlines could be reliable indicators of sex. The proximal aspect of the humerus, however, tends not to be well preserved in skeletal materials. Specifically, the humeral head is not as strong because of its trabecularis structure when compared with the humeral shaft. Thus, the methods presented here may have to be applied to other anatomical views, e.g., anterior or medial, to numerically analyze sex differences in size and shape of the proximal humeri excluding the humeral head. Finally, there is a continuing need for other size and shape studies, utilizing skeletal materials, of other limb bones, which may provide additional information useful for quantitative sex determinations.

References

1. Holman DJ, Bennett KA. Determination of sex from arm bone measurements. Am J Phys Anthropol 1991;84:421–6.
2. Steele DG. The estimation of sex on the basis of the talus and calcaneus. Am J Phys Anthropol 1976;45:581–8.
3. Schulter-Ellis FP, Hayek LA, Schmidt DJ. Determination of sex with a discriminant analysis of new pelvic bone measurements. Part II. J Forensic Sci 1985;30:178–85.
4. Schulter-Ellis FP, Schmidt DJ, Hayek LA, Craig J. Determination of sex with a discriminant analysis of new pelvic bone measurements. Part I. J Forensic Sci 1983;28:169–78.
5. Holland TD. Sex assessment using the proximal tibia. Am J Phys Anthropol 1991;85:221–7.
6. Iscan MY, Yoshino M, Kato S. Sex determination from the tibia: Standards for contemporary Japan. J Forensic Sci 1994;39:785–92.
7. Van Gerven DP. The contribution of size and shape variation to patterns of sexual dimorphism of the human femur. Am J Phys Anthropol 1972; 37:49–60.
8. DiBennardo R, Taylor JV. Multiple discriminant function analysis of sex and race in the postcranial skeleton. Am J Phys Anthropol 1983;61: 305–14.
9. Arsuaga JL, Carretero JM. Multivariate analysis of the sexual dimorphism of the hip bone in a modern human population and in early hominids. Am J Phys Anthropol 1994;93:241–57.
10. Lestrel PE, editor. Fourier descriptors and their biological applications. Cambridge: Cambridge University Press, 1997.
11. Lestrel PE, Kimbel WH, Prior FW, Fleischmann ML. Size and shape of the hominoid distal femur: Fourier analysis. Am J Phys Anthropol 1977;46:281–90.
12. Lestrel PE. Some approaches toward the mathematical modeling of the craniofacial complex. J Craniofac Genet Dev Biol 1989;9:77–91.
13. Inoue M. Fourier analysis of the forehead shape of skull and sex determination by use of computer. Forensic Sci Int 1990;47:101–12.
14. Ferrario VF, Sforza C, Schmitz JH, Miani AJ, Taroni G. Fourier analysis of human soft tissue facial shape: sex differences in normal adults. J Anat 1995;187:593–602.

15. Lestrel PE, Engstrom C, Chaconas SJ, Bodt A. A longitudinal study of the human nasal bone in *Norma Lateralis:* Size and shape considerations. In: Dixon AD, Sarnat BG, Hoyte DAN, editors. Fundamentals of bone growth: Methodology and applications. Boca Raton: CRC Press, 1991;547–64.
16. Lestrel PE. Method for analyzing complex two-dimensional forms: Elliptical Fourier functions. Am J Hum Biol 1989;1:149–64.
17. Kuhl FP, Giardina CR. Elliptic Fourier features of a closed contour. Comp Graph Imag Proc 1982;18:236–58.
18. Lestrel PE, Bodt A, Swindler DR. Longitudinal study of cranial base shape changes in *Macaca nemestrina.* Am J Phys Anthropol 1993;91: 117–29.
19. Ferson S, Rohlf FJ, Koehn RK. Measuring shape variation of two dimensional outlines. Syst Zool 1985;34:59–68.
20. Rohlf FJ, Archie JW. A comparison of Fourier methods for the description of wing shape in mosquitoes (*Diptera: culicidae*). Syst Zool 1984;33:302–17.
21. Tanaka H. Numerical analysis of the proximal humeral outline: Bilateral shape differences. Am J Hum Biol 1999;11:343–57.
22. France DL. Osteometry at muscle origin and insertion in sex determination. Am J Phys Anthropol 1988;76:515–26.
23. Takayama H. An examination of photographic measurement in craniology. J Anthrop Soc Nippon 1980;88:249–68.
24. Wolfe CA, Lestrel PE, Read DW. EFF23: 2-D and 3-D Elliptical Fourier functions. Sylmer: C. Wolfe Consulting Software Engineering, 1996.
25. Giardina CR, Kuhl FP. Accuracy of curve approximation by harmonically related vectors with elliptical loci. Comp Graph Imag Proc 1977;6: 277–85.
26. Martin R, Knussmann R. Anthropologie—Handbuch der vergleichenden Biologie des Menschen. Stuttgart: Gustav Fischer Verlag, 1988 (in German).
27. Tagaya A. Development of a generalized discriminant function for cross-population determination of sex from long bones of the arm and leg. J Can Soc Forensic Sci 1989;22:159–75.
28. Richman EA, Michel ME, Schulter-Ellis FP, Corruccini RS. Determination of sex by discriminant function analysis of postcranial skeletal measurements. J Forensic Sci 1979;24:159–67.
29. Itoi E, Kuechle DK, Newman SR, Morrey BF, An K. Stabilising function of the biceps in stable and unstable shoulder. J Bone Joint Surg 1993;75-B:546–50.
30. Itoi E, Newman SR, Kuechle DK, Morrey BF, An K. Dynamic anterior stabilisers of the shoulder with the arm in abduction. J Bone Joint Surg 1994;76-B:834–6.
31. Inman VT, Saunders JB, Abotto LC. Observations on the function of the shoulder joint. J Bone Joint Surg 1944;26:1–30.
32. Poppen NK, Walker PS. Forces at the glenohumeral joint in abduction. Clin Orthop 1978;135:165–70.
33. Fresia AE, Ruff CB, Larsen CS. Temporal decline in bilateral asymmetry of the upper limb on the Geogia Coast. In: Larsen CS, editor. The Archaeology of Mission Santa Catalina de Guale 2. Biocultural Interpretations of a Population in Transition: Anthropological Papers of the American Museum of Natural History, 1990;121–50.
34. Collier S. Sexual dimorphism in relation to big-game hunting and economy in modern human populations. Am J Phys Anthropol 1993;91: 485–504.

Additional information and reprint requests:
Hideyuki Tanaka, Ph.D.
Laboratory of Human Ergology
Department of Human-Computer Interaction Science
Tokyo University of Agriculture and Technology
3-5-8 Saiwai-cho, Fuchu, Tokyo 183-8509, Japan